BBA - Molecular Basis of Disease 1865 (2019) 1241–1252

Contents lists available at ScienceDirect

BBA - Molecular Basis of Disease

journal homepage: www.elsevier.com/locate/bbadis

# Fibroblast growth factor 21 protects the heart from angiotensin II-induced cardiac hypertrophy and dysfunction via SIRT1

Santie Li[a,1], Zhongxin Zhu[a,1], Mei Xue[b,1], Xinchu Yi[a], Jiaojiao Liang[c], Chao Niu[a], Gen Chen[a], Yingjie Shen[a], Hongping Zhang[d], Jiayong Zheng[d], Congcong Zhao[a], Yangzhi Liang[a], Weitao Cong[a], Yang Wang[c,*], Litai Jin[a,*]

[a] School of Pharmaceutical Science, Wenzhou Medical University, Wenzhou, PR China
[b] Precision Medicine Center, The First Affiliated Hospital of Wenzhou Medical University, Wenzhou, PR China
[c] Department of Histology and Embryology, Institute of Neuroscience, Wenzhou Medical University, Wenzhou, PR China
[d] People's Hospital of Wenzhou, Wenzhou, PR China

ARTICLE INFO

*Keywords:*
Fibroblast growth factor 21
Angiotensin II
Cardiac hypertrophy
SIRT1
AMPK
FoxO1

ABSTRACT

*Aims:* This study investigated the mechanism through which fibroblast growth factor 21 (FGF21) protects against angiotensin II (Ang II)-induced cardiac hypertrophy and dysfunction.

*Methods:* Male silent information regulator 1 (SIRT1) flox/flox and cardiomyocyte-specific inducible SIRT1 knockout mice (SIRT1-iKO) were generated and treated with Ang II (1.1 mg/kg/day for 4 weeks) at the age of 8–12-week-old. FGF21 treatment [2.5 mg/kg/day for 4 weeks by intraperitoneal (i.p.) injection] was initiated at the same time as the Ang II infusion. For in vitro studies, neonatal rat cardiomyocytes (NRCMs), H9c2 rat cardiomyocytes and isolated adult mouse cardiomyocytes were treated with Ang II (1 μM) and FGF21 (20 nM) for 24 h with or without SIRT1 silencing.

*Results:* FGF21 treatment significantly attenuated Ang II-induced cardiac hypertrophy and dysfunction. SIRT1 knockout abolished the ability of FGF21 to prevent Ang II-induced cardiac hypertrophy, fibrosis, and apoptosis, without affecting the beneficial effects of FGF21 in Ang II-induced hypertension, and did not influence the hypertension itself. FGF21 markedly increased the deacetylase activity of SIRT1 and promoted the interaction of SIRT1 with liver kinase B1 (LKB1) and forkhead box protein O1 (FoxO1), resulting in decreased acetylation of these SIRT1 target proteins. Consequently, FGF21 promoted the activation of the LKB1 target adenosine monophosphate-activated protein kinase (AMPK) and altered the transcriptional activity of FoxO1 on its downstream target genes catalase (*Cat*), MnSOD (*Sod2*), and *Bim*, resulting in reduced reactive oxygen species (ROS) accumulation and cardiomyocyte apoptosis.

*Conclusions:* FGF21 improves cardiac function and alleviates Ang II-induced cardiac hypertrophy in a SIRT1-dependent manner.

## 1. Introduction

Pathological cardiac hypertrophy induced by hypertension or other stimuli is a leading cause of morbidity and mortality worldwide [1]. During the development of cardiac hypertrophy, the heart progresses from concentric hypertrophy to eccentric hypertrophy. This leads to cardiac fibrosis and cardiomyocyte apoptosis and finally to heart failure, which is often fatal [2]. Thus, it is important to identify mechanisms through which pathological cardiac hypertrophy could be targeted therapeutically.

Fibroblast growth factor 21 (FGF21) is an effective metabolic regulator that controls glucose and lipid homeostasis [3]. The liver and adipose tissue are the main sites of FGF21 production and secretion [4]. Recent studies showed that skeletal muscle and the heart are also important sources and targets of FGF21 [5,6]. Notably, FGF21 has been shown to protect the heart from isoproterenol-induced cardiac hypertrophy in mice [6]. However, the effects of FGF21 on angiotensin II (Ang II) infusion-induced cardiac hypertrophy and dysfunction have not been demonstrated.

Silent information regulator 1 (SIRT1), a class III histone

* Corresponding authors.
*E-mail addresses:* yw1867@126.com (Y. Wang), jin_litai@126.com (L. Jin).
[1] These authors contributed equally to this work.

https://doi.org/10.1016/j.bbadis.2019.01.019
Received 31 July 2018; Received in revised form 29 December 2018; Accepted 16 January 2019
Available online 21 January 2019
0925-4439/ 

deacetylase, is a member of the sirtuin family, which includes SIRT1–SIRT7. SIRT1 plays an important role in the regulation of tissue homeostasis by deacetylating downstream target proteins involved in this process [7]. Of note, the effects of FGF21 are strongly correlated with SIRT1 activity [8]. Previous studies showed that SIRT1 can reduce inflammatory responses by deacetylating NF-κB/p65, downregulate apoptosis by deacetylating p53, and promote mitochondrial biogenesis by deacetylating peroxisome proliferator-activated receptor-γ coactivator-1α (PGC-1α) [9–11]. SIRT1 has also been shown to regulate energy metabolism through adenosine monophosphate-activated protein kinase (AMPK) by deacetylating liver kinase B1 (LKB1) [12]. In mice, during embryonic development, SIRT1 is highly expressed in the heart, and knockout of SIRT1 inhibits cardiac development [13]. In adult mice, however, cardiomyocyte-specific inducible knockout of SIRT1 has no adverse effects on basal cardiac function [14]. However, under pathological conditions, such as oxidative stress, endoplasmic reticulum stress, inflammation, hypoxia, or aging, these mice exhibit poor resistance to diseases and develop more severe symptoms, with a much higher mortality rate [14–16].

In this study, adult mice with a cardiac-specific inducible knockout of SIRT1 (SIRT1-iKO) were used to test the effect of exogenous administration of FGF21 on Ang II-induced cardiac hypertrophy and dysfunction. Using these animals along with in vitro cell models, we observed that the protective effects of FGF21 on cardiac dysfunction were dependent on SIRT1-mediated AMPK activation and regulation of FoxO1-dependent transcription.

## 2. Materials and methods

### 2.1. Animals

SIRT1 flox/flox mice on C57BL/6 background were generated as previously described [17]. Mice with tamoxifen-inducible Cre-fusion protein under the control of the cardiomyocyte-specific α-myosin heavy-chain promoter (αMHC-MerCreMer) were previously described [18]. αMHC-MerCreMer transgenic mice were crossed to SIRT1 flox/flox mice to deplete SIRT1 expression in adult cardiomyocytes under tamoxifen administration. For SIRT1 flox/flox mice and SIRT1 flox/flox crossed with αMHC-MerCreMer mice, tamoxifen (Santa Cruz Biotechnology, sc-208,414) was administered at the dose of 75 mg/kg/day for 5 consecutive days by intraperitoneal (i.p.) injection. After the injection, all mice were kept for a 7-day waiting period to get the efficient gene knockout. Genotypes of the transgenic mice were detected by polymerase chain reaction (PCR) analysis using the DNA from mouse tail and the specific primers were used as follows:

αMHC-MerCreMer
Forward: 5′-GCGGTCTGGCAGTAAAAACTATC-3′
Reverse: 5′-GTGAAACAGCATTGCTGTCACTT-3′
SIRT1
Forward: 5′-GGTTGACTTAGGTCTTGTCTG-3′
Reverse: 5′-CGTCCCTTGTAATGTTTCCC-3′

For SIRT1 flox/flox and SIRT1-iKO mice (8–12-week-old), ALZET® Osmotic Pumps (Model 2004) containing PBS or Ang II (Santa Cruz Biotechnology, sc-363,643) were implanted subcutaneously and were calibrated to release the drug at the dose of 1.1 mg/kg/day for 28 days. Recombinant human FGF21 (produced by Wenzhou Medical University gene engineering laboratory) were administered by i.p. injection at the dose of 2.5 mg/kg/day for 28 days following the implantation of the minipumps.

All mice were housed in temperature-controlled environment with free access to food and water under 12-h light/dark cycles. All experimental procedures were approved by the Institutional Animal Care and Use Committee of Wenzhou Medical University.

### 2.2. Cell culture and cardiomyocytes isolation

Neonatal rat cardiomyocytes (NRCMs) from 1 to 3-day-old Sprague–Dawley rats were isolated by using a series of collagenase (Collagenase Type II, Gibco, 17,101,015) digestions, cells were then collected by centrifugation and cardiac fibroblasts were removed after a 1-h pre-plating step. NRCMs were cultured in Dulbecco's modified Eagle's medium (DMEM) supplemented with 10% FBS and 1% penicillin/streptomycin in an incubator containing 95% air and 5% $CO_2$ at 37 °C.

H9c2 rat cardiomyocytes were purchased from the American Type Cell Collection (ATCC) and were cultured in DMEM supplemented with 10% FBS and 1% penicillin/streptomycin in an incubator containing 95% air and 5% $CO_2$ at 37 °C.

Adult mouse cardiomyocytes from 8 to 12 weeks old C57BL/6 mice were isolated as previously described [18] and were cultured in medium 199 (M199) supplemented with 10% FBS and 1% penicillin/streptomycin in an incubator containing 95% air and 5% $CO_2$ at 37 °C.

For RNA interference, cells were transfected with SIRT1 siRNA (Santa Cruz Biotechnology, sc-108043) or control scramble siRNA (Santa Cruz Biotechnology, sc-37007) by Lipofectamine 3000 for 12 h in Opti-MEM. After the transfection, cells were removed to full-growth medium for another 12 h and then were analyzed for further studies. Cardiomyocytes were treated with Ang II (1 μM) for 24 h in the presence or absence of FGF21 (20 nM).

### 2.3. Echocardiography

At the end of the animal study, all mice were fasted for 8 h and then were anesthetized by 2% isoflurane. Imaging was captured with a Visual Sonics Vevo 770 High-Resolution Imaging System. The echocardiographer was blinded to the different genotypes. The following cardiac parameters were measured: left ventricular end diastolic diameter (LVEDD), left ventricular end systolic diameter (LVESD), left ventricular posterior wall thickness in diastole (LVPWd), left ventricular ejection fraction (EF%) and fractional shortening (FS%).

### 2.4. Blood pressure measurement

Blood pressure was measured by tail-cuff system (BP 2000, Visitech Systems) in conscious mice at day time (2:00 p.m. to 5:00 p.m.), at least 20 constant measurements were recorded to obtain the final result.

### 2.5. Heart section histology

Mouse hearts were harvested and fixed in 4% paraformaldehyde, embedded in paraffin after dehydration, and then sectioned at 5 μm. After deparaffinization, those sections were stained with hematoxylin-eosin (H&E) staining for the detection of cardiac morphology, and picro sirius red (PSR) staining for the detection of cardiac fibrosis. Pictures were taken by a Nikon Eclipse Ni light microscopy.

### 2.6. TUNEL staining

Terminal deoxynucleotidyl transferase-mediated FITC-dUTP nick end labeling (TUNEL) staining was performed using the DeadEnd™ Fluorometric TUNEL System (Promega, G3250) according to the manufacturer's protocols. For the heart tissues, paraffin embedded sections (5 μm) were stained with TUNEL for apoptotic cells and DAPI for all the nuclei. For H9c2 cardiomyocytes, different groups of cells were fixed by 4% paraformaldehyde for 15 min at room temperature, and then were stained with TUNEL and DAPI for the detection of apoptosis. The images were captured using a Leica SP8 confocal microscopy.

**Table 1**
Details of the primers used in the RT-PCR analysis.

| Primer | Forward | Reverse |
|---|---|---|
| Rat *Anp* | 5′-GGGGGTAGGATTGACAGGAT-3′ | 5′-CTCCAGGAGGGTATTCACCA-3′ |
| Rat *Bnp* | 5′-ACAATCCACGATGCAGAAGCT-3′ | 5′-GGGCCTTGGTCCTTTGAGA-3′ |
| Rat *Myh7* | 5′-CCTCGCAATATCAAGGGAAA-3′ | 5′-TACAGGTGCATCAGCTCCAG-3′ |
| Rat *GAPDH* | 5′-ATCAAGAAGGTGGTGAAGCA-3′ | 5′-AAGGTGGAAGAATGGGAGTTG-3′ |
| Mouse *Col1A* | 5′-CCCAAGGAAAAGAAGCACGTC-3′ | 5′-AGGTCAGCTGGATAGCGACATC-3′ |
| Mouse *Col3A* | 5′-TGGTAGAAAGGACACAGAGGC-3′ | 5′-TCCAACTTCACCCTTAGCACC-3′ |
| Mouse *Fn1* | 5′-TTAAGCTCACATGCCAGTGC-3′ | 5′-TCGTCATAGCACGTTGCTTC-3′ |
| Mouse *Anp* | 5′-CCTAAGCCCTTGTGGTGTGT-3′ | 5′-CAGAGTGGGAGAGGCAAGAC-3′ |
| Mouse *Bnp* | 5′-CTGAAGGTGCTGTCCCAGAT-3′ | 5′-CCTTGGTCCTTCAAGAGCTG-3′ |
| Mouse *Myh7* | 5′-ATCAATGCAACCCTGGAGAC-3′ | 5′-CGAACATGTGGTGGTTGAAG-3′ |
| Mouse *Cat* | 5′-CACTGACGAGATGGCACACTTTG-3′ | 5′-TGGAGAACCGAACGGCAATAGG-3′ |
| Mouse *SOD2* | 5′-GCCTCCCAGACCTGCCTTAC-3′ | 5′-GTGGTACTTCTCCTCGGTGGCG-3′ |
| Mouse *Bim* | 5′-CGGATCGGAGACGAGTTCA-3′ | 5′-TTCAGCCTCGCGGTAATCA-3′ |
| Mouse *FGF21* | 5′-GTGTCAAAGCCTCTAGGTTTCTT-3′ | 5′- GGTACACATTGTAACCGTCCTC-3′ |
| Mouse *GAPDH* | 5′-AGGTCGGTGTGAACGGATTTG-3′ | 5′-TGTAGACCATGTAGTTGAGGTCA-3′ |

### 2.7. DHE staining

Dihydroethidium (DHE) (Thermo Fisher Scientific, D11347) staining was performed as previously described [19]. Cardiac sections (5 μm) and H9c2 cardiomyocytes were stained with DHE to monitor the generation of reactive oxygen species (ROS). Pictures were captured using a Leica SP8 confocal microscopy.

### 2.8. Immunofluorescence staining

NRCMs were fixed in 4% paraformaldehyde for 15 min and then were permeabilized in 0.1% Triton X-100 for 20 min at room temperature. Cardiomyocytes were then blocked in PBS containing 0.5% bovine serum albumin and incubated with anti-Cardiac Troponin T antibody (1:200) (Abcam, ab8295) at 4 °C overnight followed by secondary antibody conjugated with FITC. Finally, the nuclei were stained with DAPI. Images were visualized and captured with a Leica SP8 confocal microscopy.

### 2.9. Immunological assay

Serum FGF21 concentrations were measured by using a mouse-specific FGF21 ELISA kit (CUSABIO, CSB-EL008627MO) according to the manufacturer's protocols.

### 2.10. Western blotting and antibodies

Equal amounts of protein lysates from cardiac tissues or cardiomyocytes were separated by SDS-PAGE and transferred to PVDF membrane (Merck Millipore, IPVH00010), then subjected to western blotting analysis for: TGF-β1 (Abcam, ab64715), α-SMA (Abcam, ab23575), p-mTOR (Ser2448) (CST, 2971), mTOR (CST, 2983), p-Akt (Ser473) (CST, 4060), Akt (CST, 4691), p-GSK3β (Ser9) (CST, 9323), GSK3β (CST, 9315), p-Erk1/2 (Thr202/Tyr204) (CST, 9101), Erk1/2 (CST, 9102), p-JNK (Thr183/Tyr185) (CST, 4668), JNK (CST, 9252), Bax (Abcam, ab32503), Bcl-2 (Abcam, ab59348), c-caspase-3 (CST, 9661), p-AMPKα (Thr172) (CST, 2535), AMPKα (CST, 2603), SIRT1 (CST, 8469), LKB1 (Santa Cruz Biotechnology, sc-32,245), acetylated-lysine (CST, 9441), acetylated-FoxO1 (Santa Cruz Biotechnology, sc-49,437), FoxO1 (CST, 2880), catalase (Abcam, ab1877), MnSOD (CST, 13141), Bim (CST, 2933), 3-Nitrotyrosine (Millipore, 05–233), GAPDH (CST, 5174). Proteins were visualized using an Image Quant LAS 4000 (GE Healthcare) system, and the secondary antibodies are: goat anti-rabbit HRP (Bio-Rad, 1,706,515), goat anti-mouse HRP (Bio-Rad, 1,706,516).

### 2.11. Co-immunoprecipitation

Cell lysates with 500 μg proteins were incubated with 20 μL PureProteome™ Protein A/G Mix Magnetic Beads (Merck Millipore, LSKMAGAG10) and appropriate primary antibodies at 4 °C overnight according to the manufacturer's protocols. The supernatants of the immunoprecipitates were subjected to immunoblotting for the detection of protein-protein interaction.

### 2.12. SIRT1 activity measurement

The deacetylase activity of SIRT1 was measured by SIRT1 Activity Assay Kit (Fluorometric) (Abcam, ab156065) according to the manufacturer's protocols.

### 2.13. Reverse transcriptase-polymerase chain reaction (RT-PCR)

Total RNA from heart tissues or cells were isolated by Trizol reagent (BioTeke, RP1001) and reversely transcribed into complementary DNA (cDNA) using the GoScript™ Reverse Transcription System (Promega, A5001) according to the manufacturer's protocols. GAPDH was used as a loading control. The specific primers are shown in Table 1.

### 2.14. Statistical analysis

Data were analyzed by GraphPad Prism 5.0 and results were expressed as mean ± standard error of the mean (S.E.M.). Differences of each sample were evaluated using the unpaired Student's two-tailed *t*-test or analysis of variance (ANOVA). A value of $P < 0.05$ was considered significant. All experiments were repeated at least three times.

## 3. Results

### 3.1. FGF21 treatment alleviates Ang II-induced cardiac hypertrophy in a SIRT1-dependent manner

To investigate the effect of long-term FGF21 treatment on Ang II-induced cardiac hypertrophy, SIRT1 flox/flox mice and SIRT1-iKO mice were generated (Fig. S1A, B), and age-matched, 8–12-week-old male mice were subjected to sustained Ang II infusion for 4 weeks. FGF21 treatment was initiated at the same time as the Ang II infusion. Echocardiography showed that SIRT1 flox/flox mice developed concentric hypertrophy after the Ang II infusion, as evidenced by a compensatory increase in the EF% and FS%, while those increases were blunted by FGF21 treatment (Fig. 1A, B). By contrast, in SIRT1-iKO mice, FGF21 treatment had no effect on the EF% or the FS% in Ang II infusion-induced eccentric hypertrophy (Fig. 1A, B). Furthermore,

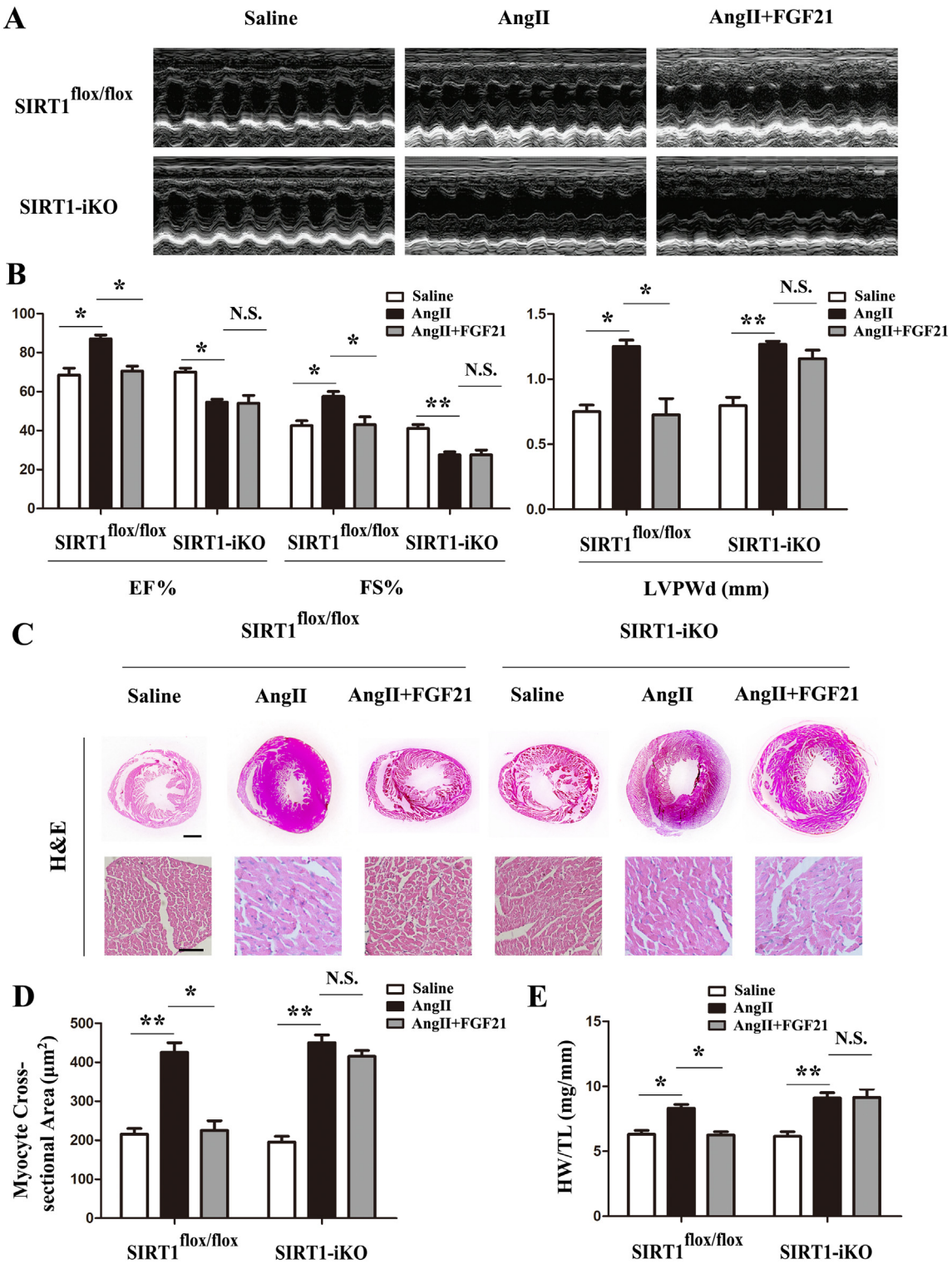


**Fig. 1.** FGF21 alleviates Ang II-induced cardiac hypertrophy in a SIRT1-dependent manner.
A) Representative M-mode echocardiographic recording obtained from SIRT1 flox/flox mice and SIRT1-iKO mice receiving FGF21 or vehicle treatment with saline infusion or Ang II infusion for 28 days. B) Quantitative changes in EF%, FS%, and LVPWd were compared between different groups. Data are mean ± SEM for n = 6 mice in each group. C) H&E staining for whole heart sections (Scale bar = 1 mm, upper panel) and histological examination of myocardium (Scale bar = 50 μm, lower panel) in SIRT1 flox/flox mice and SIRT1-iKO mice receiving FGF21 or vehicle treatment with saline infusion or Ang II infusion for 28 days. D) Quantification of cardiomyocyte size in different groups of mice. Data are mean ± SEM for n = 6 mice in each group. E) Quantification of HW/TL ratios in different groups of mice. Data are mean ± SEM for n = 6 mice in each group. *$P < 0.05$, **$P < 0.01$, N.S., not significant.

echocardiography and histological analysis by H&E staining revealed that FGF21 alleviated Ang II-induced ventricular and cardiomyocyte hypertrophy in SIRT1 flox/flox mice but not in SIRT1-iKO mice (Fig. 1B–D). In addition, similar effects were observed for the ratio of the heart weight to the tibia length (HW/TL ratio) and the mRNA levels of the hypertrophic genes *Anp*, *Bnp*, and *Myh7* (Figs. 1E, S2A).

To confirm the effects of FGF21/SIRT1 on Ang II-induced cardiac hypertrophy in vitro, NRCMs were treated with Ang II/FGF21 in the absence or presence of SIRT1 siRNA. Cardiac Troponin T immunofluorescence was performed to obtain the clear-cut assessment of cellular hypertrophy. *Anp*, *Bnp*, and *Myh7* mRNA levels were also measured as indicators of cellular hypertrophy. Consistent with the in vivo results, the capacity of FGF21 to attenuate Ang II-induced cardiomyocyte hypertrophy was significantly restricted after transfection with SIRT1-specific siRNA (Fig. S2B, C).

Furthermore, as FGF21 has been proved to prevent Ang II-induced hypertension largely by improving vascular dysfunction [20], we therefore evaluated the blood pressure in our animal models. As shown in Fig. S3A and B, FGF21 attenuated the increase of systolic and diastolic blood pressure caused by Ang II infusion in both SIRT1 flox/flox and SIRT1-iKO mice, suggesting in SIRT1-iKO mice FGF21 could still protect the vascular system. In addition, there is no significant difference in the blood pressure between SIRT1 flox/flox and SIRT1-iKO mice treated with Ang II. This reminds us that cardiomyocyte SIRT1 is not involved in the hypertensive action of Ang II. Meanwhile, previous study has demonstrated that SIRT1 controls cardiac FGF21 expression and protects it from oxidative stress [6], and Ang II-induced hypertension is related with increased circulating levels of FGF21 [20]. Thereby, we measured FGF21 levels in both the serum and the cardiac tissues. Results shown that Ang II treatment caused a largely elevation of serum FGF21, without significant difference between SIRT1 flox/flox and SIRT1-iKO mice (Fig. S3C), proving that the heart is not the main source of FGF21 secretion in this mode. In contrast, SIRT1 deletion in the cardiac tissues could greatly decrease the mRNA expression of FGF21 both in normal and pathological conditions (Fig. S3D).

### 3.2. FGF21 treatment inhibits Ang II-induced cardiac fibrosis in a SIRT1-dependent manner

PSR staining was performed to assess myocardial interstitial and perivascular fibrosis. As shown in Fig. 2A and B, FGF21 attenuated Ang II-induced interstitial and perivascular fibrosis in SIRT1 flox/flox mice, but in SIRT1-iKO mice, there was no significant difference in the extent of interstitial or perivascular fibrosis in FGF21-treated or vehicle-treated hypertrophied hearts. Cardiac fibrosis can be induced by several molecular signals, chiefly the fibrotic cytokine transforming growth factor-beta 1 (TGF-β1) [21]. The cardiac levels of TGF-β1 and the myofibroblast marker α-smooth muscle actin (α-SMA) were therefore measured. As shown in Fig. 2C–E, both TGF-β1 and α-SMA were markedly increased after Ang II infusion and were reduced by FGF21 treatment in SIRT1 flox/flox mice but not in SIRT1-iKO mice. Furthermore, the mRNA levels of collagen type I alpha (*Col1A*), collagen type III alpha (*Col3A*), and fibronectin (*Fn1*) were measured in cardiac tissue samples harvested after Ang II/FGF21 treatment. As shown in Fig. S3E, Ang II increased the expression of *Col1A*, *Col3A*, and *Fn1* in both SIRT1 flox/flox and SIRT1-iKO mice, while FGF21 alleviated the expression of these fibrosis-related genes in SIRT1 flox/flox mice but not in SIRT1-iKO mice.

### 3.3. FGF21 treatment attenuates Ang II-induced activation of the Akt and MAPK signaling pathways in a SIRT1-dependent manner

During maladaptive hypertrophy and cardiac remodeling, the mammalian target of rapamycin (mTOR)/Akt and mitogen-activated protein kinase (MAPK) signaling pathways are highly activated in the cardiac tissue [22]. Cardiomyocyte hypertrophy and cardiac fibroblast activation are both associated with Akt and MAPK signaling pathway activation. Thus, the levels of phosphorylated mTOR, Akt, glycogen synthase kinase-3β (GSK-3β), extracellular signal-related kinase 1/2 (Erk1/2), and c-Jun N-terminal kinase (JNK) were measured in SIRT1 flox/flox and SIRT1-iKO mice after Ang II infusion with or without FGF21 treatment. All of these signaling molecules were activated by Ang II infusion and were attenuated after FGF21 treatment in SIRT1 flox/flox mice, but SIRT1 deletion abolished the ability of FGF21 to reduce the activation of these signaling pathways (Fig. 3A–G).

### 3.4. FGF21 treatment inhibits Ang II-induced cardiomyocyte apoptosis and the accumulation of ROS in a SIRT1-dependent manner

Because cardiomyocyte apoptosis plays an important role in pathological cardiac hypertrophy [23], TUNEL assays were performed on myocardial samples from SIRT1 flox/flox and SIRT1-iKO mice after Ang II/FGF21 treatment. Ang II infusion induced a significant increase in apoptotic myocytes, and FGF21 protected the myocytes from apoptosis in SIRT1 flox/flox mice but not in mice in which SIRT1 was deleted (Fig. 4A, B). To further confirm these observations, levels of the pro-apoptotic molecule Bcl-2-associated X protein (Bax), the anti-apoptotic molecule Bcl-2, and cleaved caspase-3 (c-CAS-3) were measured. The ratio of Bax/Bcl-2 and the expression of c-CAS-3 were markedly increased after Ang II infusion, and were reduced by FGF21 treatment in SIRT1 flox/flox mice but not in SIRT1-iKO mice (Fig. 4C–E).

At the cellular level, TUNEL staining and western blotting analysis revealed that FGF21 notably reduced Ang II-induced apoptosis in H9c2 cardiomyocytes, as evidenced by a decrease in the number of TUNEL-positive nuclei, the Bax/Bcl-2 ratio, and the level of c-CAS-3, but in the absence of SIRT1, these protective effects of FGF21 were reduced (Fig. S4A, B).

Since one of the mechanisms through which Ang II infusion damages cardiac tissue is by inducing the release of reactive oxygen species (ROS), DHE staining was used to detect accumulated ROS in myocardial tissue and H9c2 cardiomyocytes. FGF21 prevented Ang II-induced ROS formation both in vivo and in vitro in the presence of SIRT1 (Fig. S5A, C). In addition, the increase in the expression of the oxidative stress marker 3-nitrotyrosine (3-NT) in response to Ang II was also alleviated by FGF21 treatment in SIRT1 flox/flox mice, and this anti-oxidative activity of FGF21 was reduced in SIRT1-iKO mice and SIRT1 siRNA-treated H9c2 cardiomyocytes (Fig. S5B, D).

### 3.5. FGF21 treatment increases the deacetylase activity of SIRT1 and promotes AMPK activation via LKB1 deacetylation

AMPK activation is beneficial in pathological cardiac hypertrophy [24], and the protective effects of FGF21 in cardiac hypertrophy are strongly correlated with AMPK activity [8]. Thus, we evaluated the phosphorylation of AMPK in FGF21-treated mice. As shown in Fig. 5A and B, FGF21 strongly increased the level of phosphorylated AMPK in Ang II-infused SIRT1 flox/flox mice, while in SIRT1-iKO mice, the ability of FGF21 to activate AMPK was highly reduced. As isolated cardiomyocytes reflect the physiological state of cells in vivo more accurately than the H9c2 cell line, adult mouse cardiomyocytes were isolated and transfected with SIRT1 siRNA or a scrambled control siRNA. FGF21 failed to induce AMPK activation in cardiomyocytes in which SIRT1 was knocked down with siRNA (Fig. 5C–E).

LKB1 is an important modulator of AMPK activity, and SIRT1, in turn, is a crucial upstream modulator of LKB1 acetylation [12]. Thus, the interaction between SIRT1 and LKB1 and the acetylation of LKB1 were evaluated by immunoprecipitation (IP) in isolated cardiomyocytes. As shown in Fig. 5F, FGF21 markedly enhanced the binding of SIRT1 to LKB1 and promoted its deacetylation, while in cells treated with SIRT1 siRNA, the basal level of LKB1 acetylation was much higher and did not decrease with FGF21 treatment. In addition, FGF21 greatly increased the deacetylase activity of SIRT1 both in vivo and in vitro

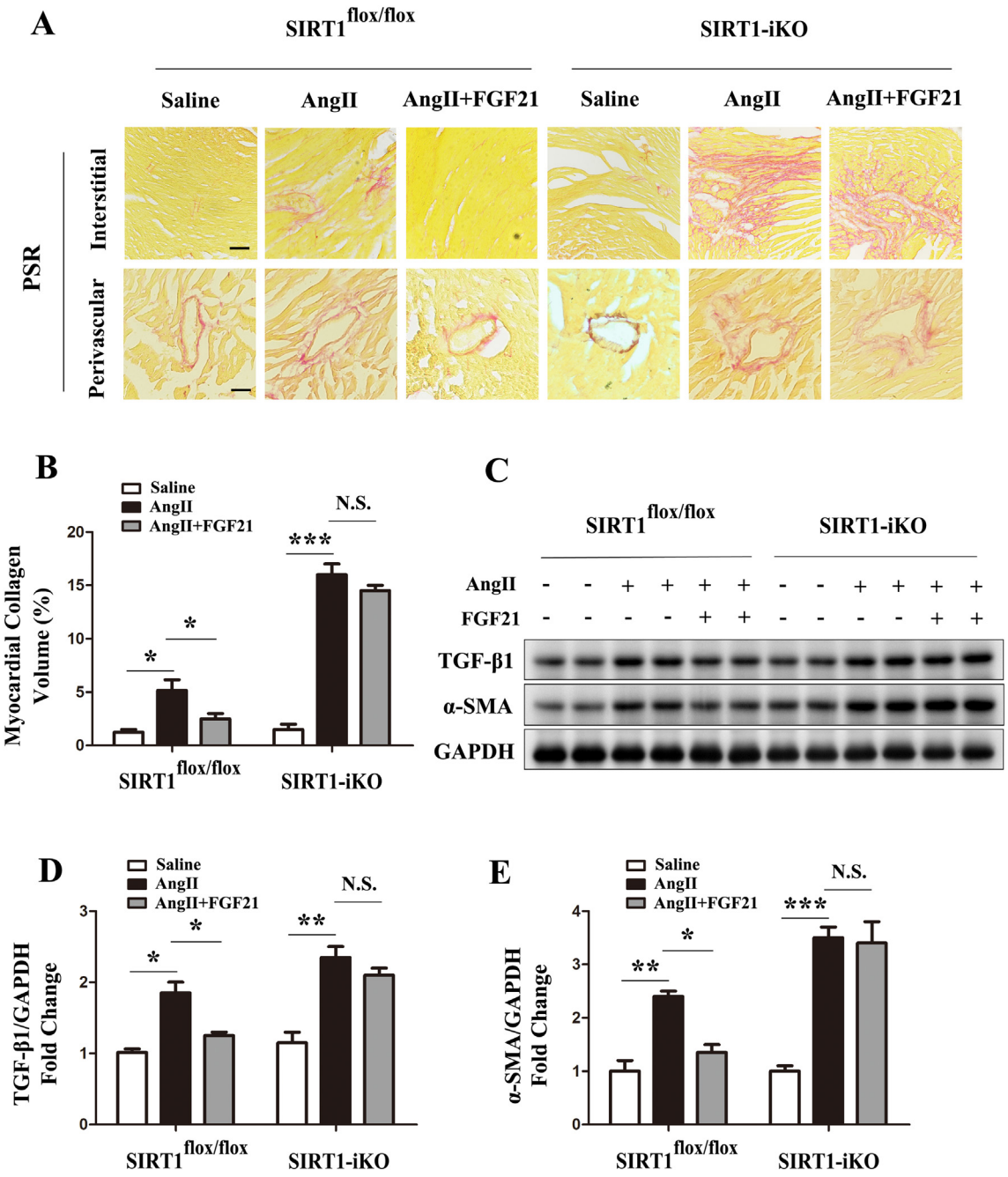


**Fig. 2.** FGF21 represses Ang II-induced cardiac fibrosis in a SIRT1-dependent manner.
A) PSR staining for the examination of interstitial and perivascular (Scale bar = 50 μm) fibrosis in SIRT1 flox/flox mice and SIRT1-iKO mice receiving FGF21 or vehicle treatment with saline infusion or Ang II infusion for 28 days. B) Quantitative changes in myocardial collagen volume were compared between different groups. Data are mean ± SEM for n = 6 mice in each group. C) Western blotting showing the expression levels of TGF-β1 and α-SMA in SIRT1 flox/flox mice and SIRT1-iKO mice receiving FGF21 or vehicle treatment with saline infusion or Ang II infusion for 28 days. GAPDH was used as a loading control. D) Quantification of TGF-β1 protein levels in different groups. Data are mean ± SEM for n = 4 mice in each group. E) Quantification of α-SMA protein levels in different groups. Data are mean ± SEM for n = 4 mice in each group. $^{*}P < 0.05$, $^{**}P < 0.01$, $^{***}P < 0.001$, N.S., not significant.

(Fig. 5G, H).

### 3.6. FGF21 treatment alters the transcriptional activity of FoxO1 through SIRT1-mediated deacetylation

Forkhead box transcription factor O1 (FoxO1) is a member of the forkhead box.

transcription factor class O subfamily. As an important downstream target of SIRT1 [25], FoxO1 has been shown to be a key player in the regulation of metabolism, apoptosis, and the oxidative stress response [26–28]. The transcriptional activity of FoxO1 is mainly regulated through post-translational modifications, such as phosphorylation, ubiquitination, and acetylation [29]. In our results, Ang II treatment increased the acetylation of FoxO1 both in vivo and in vitro. Ang II also downregulated the anti-oxidative proteins catalase and MnSOD and upregulated the pro-apoptotic protein Bim (Fig. 6A–D), all of which are transcriptional targets of FoxO1 [30,31]. As expected, FGF21 inhibited the increase in FoxO1 acetylation induced by Ang II, resulting in increased levels of catalase and MnSOD and decreased levels of Bim. However, SIRT1 deletion abolished all these beneficial effects

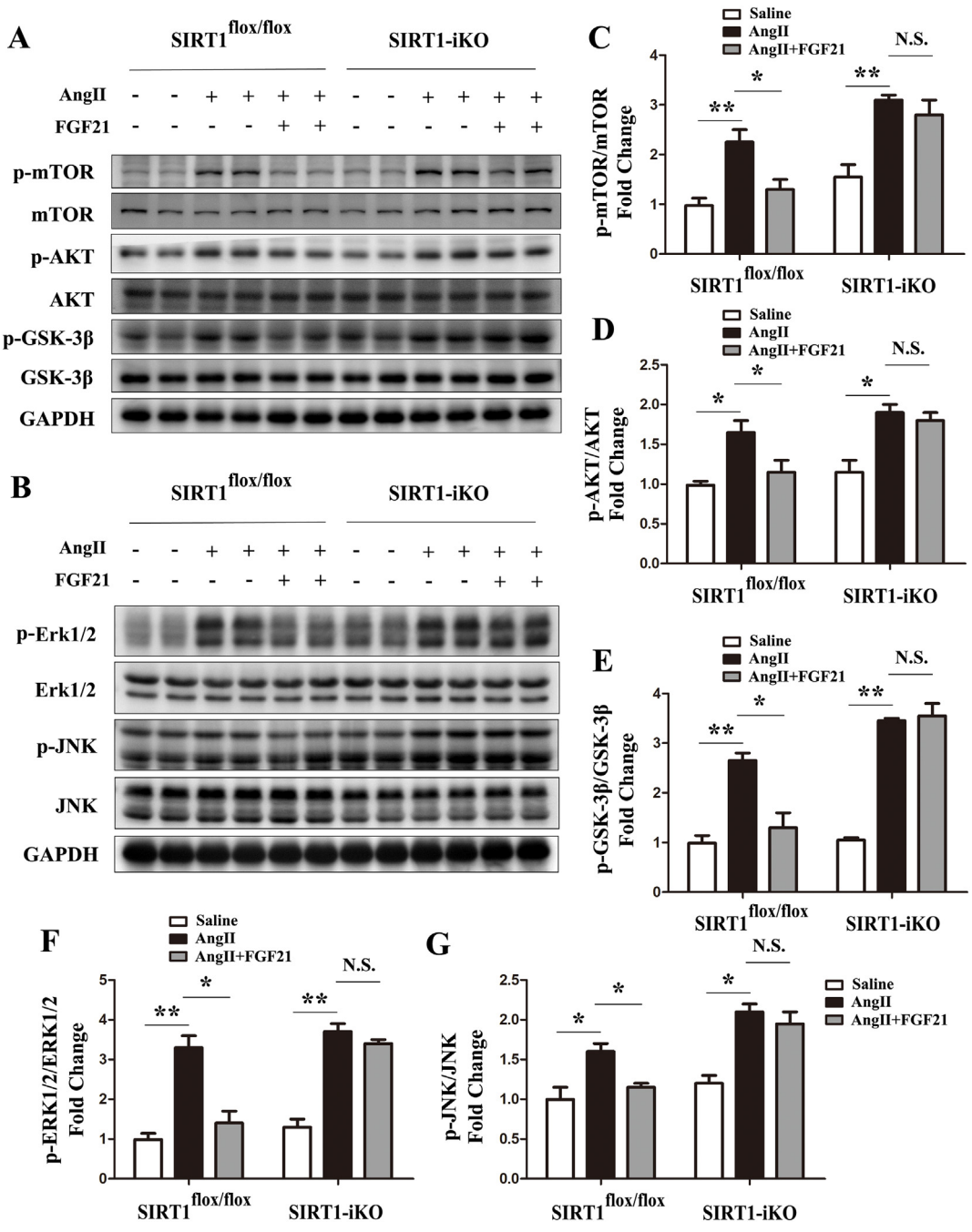


**Fig. 3.** FGF21 attenuates Ang II-induced activation of Akt and MAPK signaling pathways in a SIRT1-dependent manner.
A) Western blotting showing the expression levels of phosphorylated mTOR, Akt, and GSK3β and the total protein expression levels of mTOR, Akt, and GSK3β in SIRT1 flox/flox mice and SIRT1-iKO mice receiving FGF21 or vehicle treatment with saline infusion or Ang II infusion for 28 days. B) Western blotting showing the expression levels of phosphorylated Erk1/2 and JNK and the total protein expression levels of Erk1/2 and JNK in SIRT1 flox/flox mice and SIRT1-iKO mice receiving FGF21 or vehicle treatment with saline infusion or Ang II infusion for 28 days. C) Quantification of p-mTOR protein levels in different groups. Data are mean ± SEM for n = 4 mice in each group. D) Quantification of p-Akt protein levels in different groups. Data are mean ± SEM for n = 4 mice in each group. E) Quantification of p-GSK3β protein levels in different groups. Data are mean ± SEM for n = 4 mice in each group. F) Quantification of p-Erk1/2 protein levels in different groups. Data are mean ± SEM for n = 4 mice in each group. G) Quantification of p-JNK protein levels in different groups. Data are mean ± SEM for n = 4 mice in each group. $^{*}P < 0.05$, $^{**}P < 0.01$, N.S., not significant.

(Fig. 6A–D). Similar regulation of catalase (*Cat*), MnSOD (*Sod2*), and *Bim* mRNA levels was seen by qRT-PCR (Fig. S6A, B). IP assays also confirmed that FGF21 promoted the interaction of SIRT1 with FoxO1 in Ang II-treated isolated cardiomyocytes (Fig. 6E).

## 4. Discussion

The activation of the renin-angiotensin system (RAS) plays an important role in cardiac hypertrophy development [32]. Ang II, as the principal mediator of the RAS, can induce hypertension and thus affect cardiovascular function. Furthermore, it can directly modulate cardiomyocyte physiology, as evidenced by its effects on myocardial contractility, metabolism, and hypertrophic growth [33]. In the present studies, long-term treatment with FGF21 attenuated Ang II-induced cardiac hypertrophy and dysfunction, reduced apoptosis and fibrosis, and decreased ROS accumulation in a SIRT1-dependent manner.

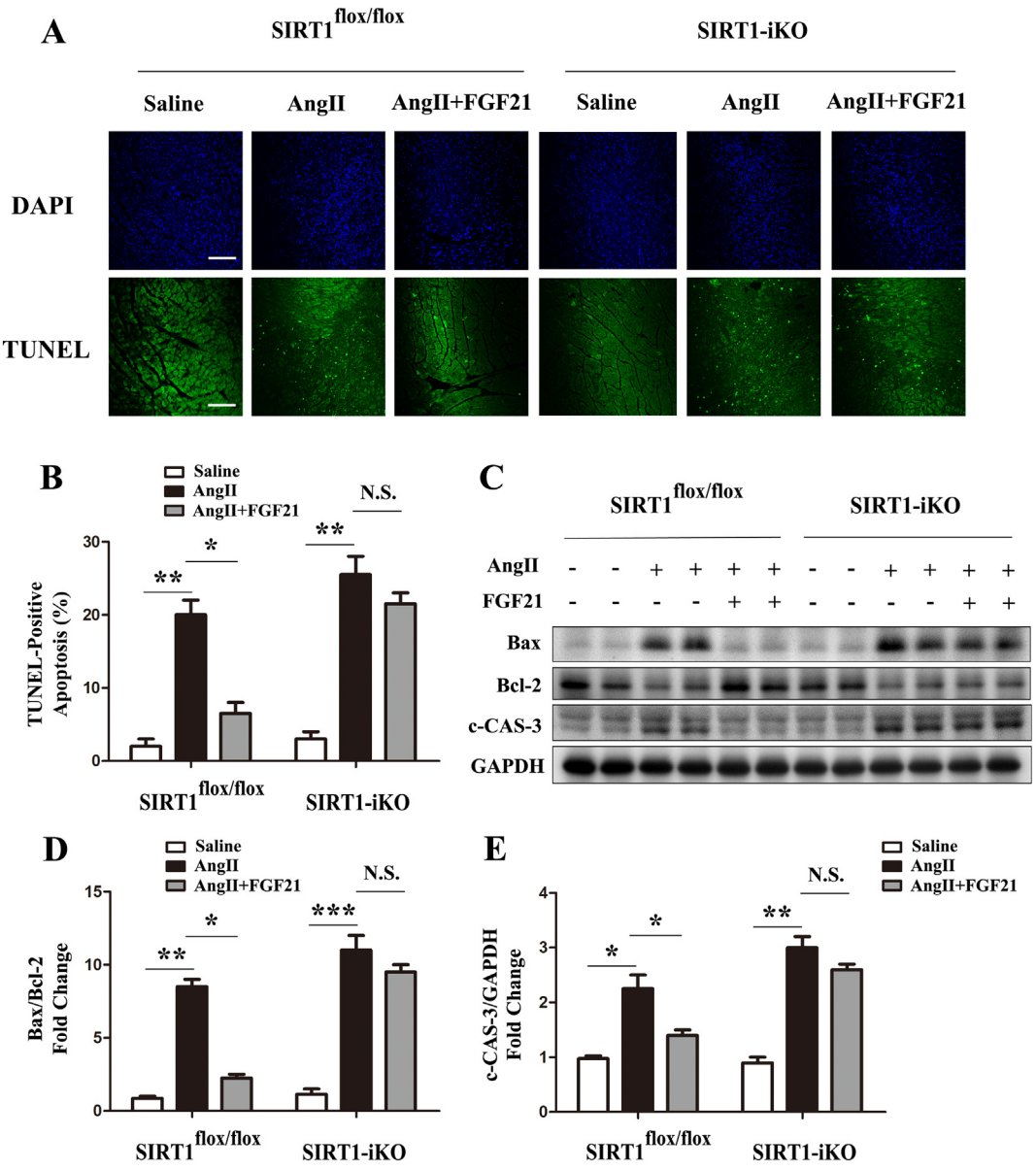


**Fig. 4.** FGF21 represses Ang II-induced cardiac apoptosis in a SIRT1-dependent manner.
A) TUNEL staining was performed on myocardial sections from SIRT1 flox/flox mice and SIRT1-iKO mice receiving FGF21 or vehicle treatment with saline infusion or Ang II infusion for 28 days. The TUNEL-positive nuclei (green) indicated the apoptotic cells. DAPI (blue) indicated all cell nuclei. Scale bar = 150 μm. B) TUNEL-positive myocyte nuclei were quantitated as a percentage of total cardiomyocyte nuclei. Data are mean ± SEM for n = 6 mice in each group. C) Western blotting showing the expression levels of Bax, Bcl-2 and c-CAS-3 in SIRT1 flox/flox mice and SIRT1-iKO mice receiving FGF21 or vehicle treatment with saline infusion or Ang II infusion for 28 days. GAPDH was used as a loading control. D) Quantification of Bax/Bcl-2 ratios in different groups. Data are mean ± SEM for n = 4 mice in each group. E) Quantification of c-CAS-3 protein levels in different groups. Data are mean ± SEM for n = 4 mice in each group. $^{*}P < 0.05$, $^{**}P < 0.01$, N.S., not significant.

Pathological cardiac hypertrophy is often associated with increased cardiomyocyte apoptosis and myocardial fibrosis, which have been proposed as principle mechanisms of heart failure [21,23,33]. The loss of cardiomyocytes through apoptosis together with activation of cardiac fibroblasts and transformation into myofibroblasts contributes to the deterioration of cardiac dysfunction and eventually leads to detrimental cardiac remodeling and heart failure [22,34]. Ang II infusion directly inhibits cardiomyocyte survival mechanisms, leading to apoptosis, and also induces the production of ROS and TGF-β1, which are the leading drivers of myocardial fibrosis [35,36]. It has previously been reported that FGF21 can alleviate cardiomyocyte apoptosis and myocardial fibrosis [37], and our results revealed that cardiomyocyte-specific SIRT1 knockout abrogated the protective effects of FGF21 in Ang II-treated mouse hearts. In SIRT1-iKO mice, FGF21 treatment did not alleviate the effects of Ang II on mTOR/Akt and MAPK signaling or ROS and TGF-β1 secretion. These results demonstrate that SIRT1 is essential for the protective effects of FGF21 in Ang II-induced pathological cardiac hypertrophy.

Previous studies showed that SIRT1 is involved in gene silencing and expression, tissue differentiation, cell survival and apoptosis, metabolism, and senescence [7]. Moreover, the upregulation of SIRT1 in cardiomyocytes can inhibit apoptosis, protect against oxidative stress, and inhibit senescence [13,14,38]. Deacetylation activity is the major function of SIRT1, a class III histone deacetylase. In this study, we found that Ang II treatment reduced SIRT1 activity, which was restored by FGF21. Increased SIRT1 activity may affect a wide range of downstream targets, including AMPK, a crucial metabolic regulator [39,40]. Once activated by phosphorylation, AMPK inhibits various anabolic

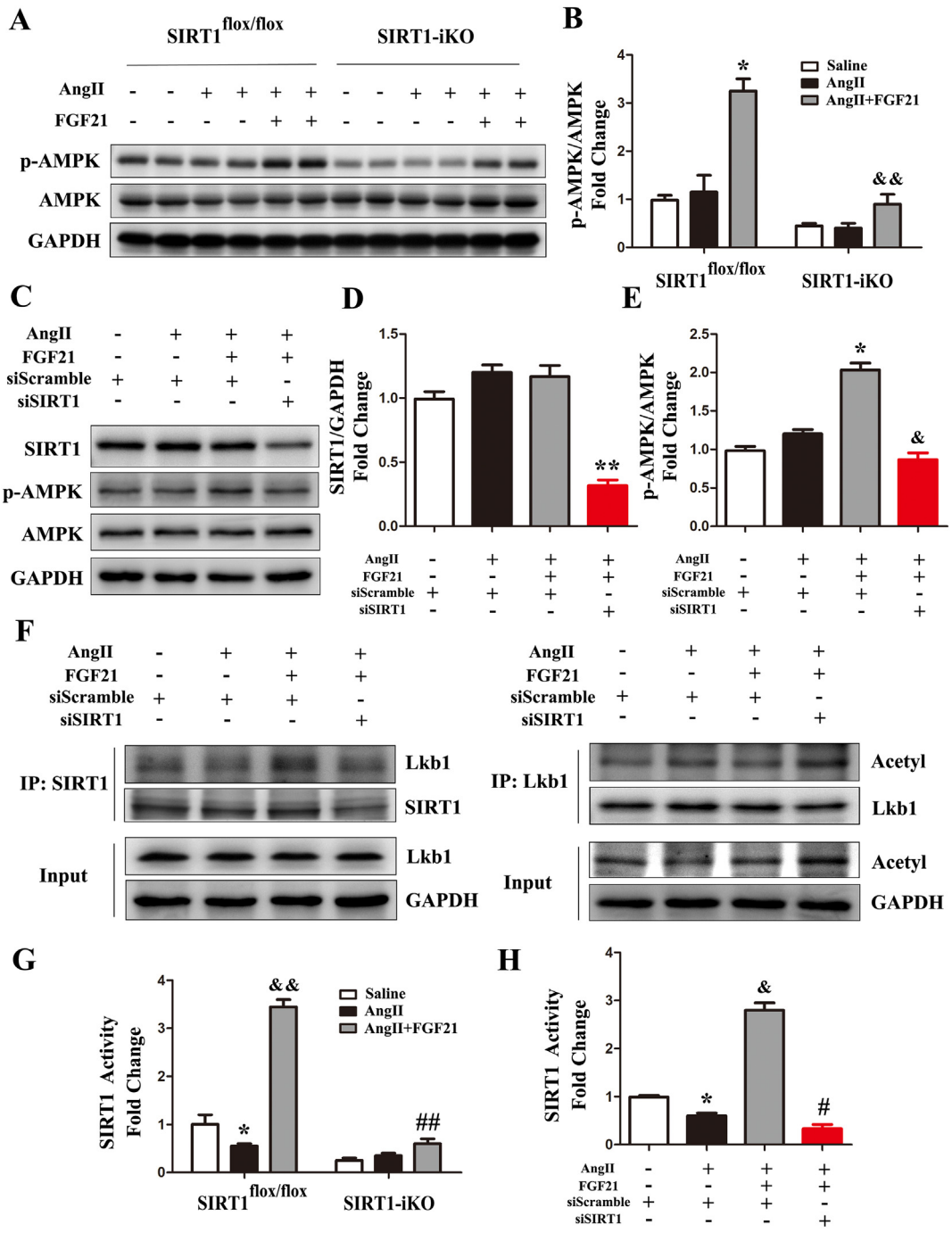


**Fig. 5.** FGF21 increases the deacetylase activity of SIRT1 and promotes AMPK activation via LKB1 deacetylation.
A) Western blotting showing the expression level of phosphorylated AMPK and the total protein expression level of AMPK in SIRT1 flox/flox mice and SIRT1-iKO mice receiving FGF21 or vehicle treatment with saline infusion or Ang II infusion for 28 days. B) Quantification of p-AMPK protein levels in different groups of mice ($^{*}P < 0.05$ versus Ang II-infused SIRT1 flox/flox mice, $^{\&\&}P < 0.01$ versus FGF21 treated Ang II-infused SIRT1 flox/flox mice). Data are mean ± SEM for n = 4 mice in each group. C) Western blotting showing the expression level of phosphorylated AMPK and the total protein expression levels of AMPK and SIRT1 in Ang II treated isolated cardiomyocytes transfected with SIRT1 siRNA or control siRNA followed by treatment with or without FGF21. GAPDH was used as a loading control. D) Quantification of SIRT1 protein levels in different groups of isolated cardiomyocytes ($^{**}P < 0.01$ versus Ang II and FGF21 treated isolated cardiomyocytes transfected with control siRNA). E) Quantification of p-AMPK protein levels in different groups of isolated cardiomyocytes ($^{*}P < 0.05$ versus Ang II treated isolated cardiomyocytes transfected with control siRNA, $^{\&}P < 0.01$ versus Ang II and FGF21 treated isolated cardiomyocytes transfected with control siRNA). F) Immunoprecipitation assays showing the interaction of SIRT1 and LKB1 and the acetylation level of LKB1 in Ang II treated isolated cardiomyocytes transfected with SIRT1 siRNA or control siRNA followed by treatment with or without FGF21. G) Measurements of the deacetylase activity of SIRT1 in different groups of mice ($^{*}P < 0.05$ versus saline-infused SIRT1 flox/flox mice, $^{\&\&}P < 0.01$ versus Ang II-infused SIRT1 flox/flox mice, $^{\#\#}P < 0.01$ versus FGF21 treated Ang II-infused SIRT1 flox/flox mice). H) Measurements of the deacetylase activity of SIRT1 in different groups of isolated cardiomyocytes ($^{*}P < 0.05$ versus isolated cardiomyocytes transfected with control siRNA, $^{\&}P < 0.05$ versus Ang II treated isolated cardiomyocytes transfected with control siRNA, $^{\#}P < 0.05$ versus Ang II and FGF21 treated isolated cardiomyocytes transfected with control siRNA).

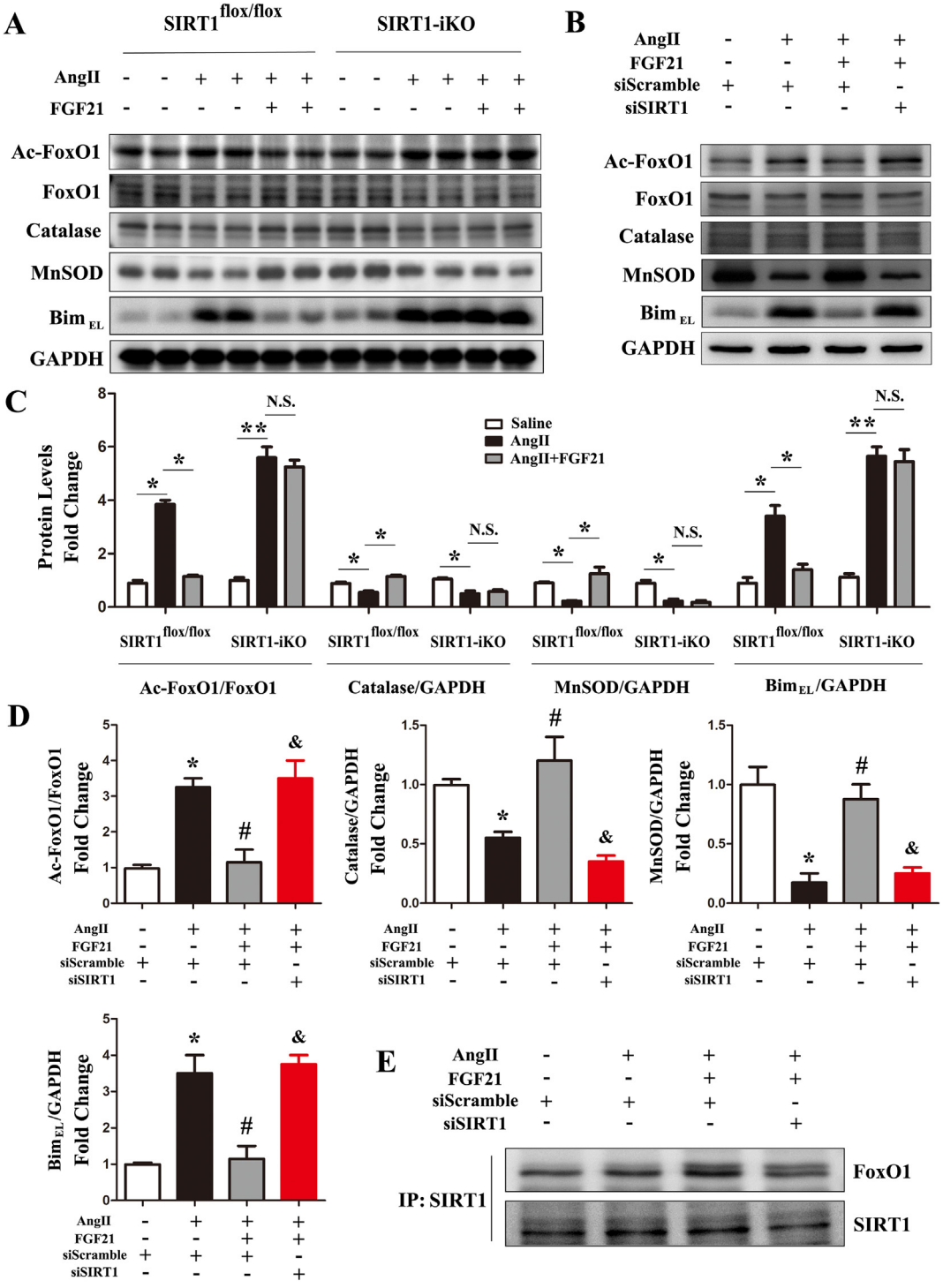


**Fig. 6.** FGF21 alters the transcriptional effects of FoxO1 through SIRT1-mediated deacetylation.
A) Western blotting showing the expression levels of acetylated-FoxO1, total FoxO1, Catalase, MnSOD and Bim in SIRT1 flox/flox mice and SIRT1-iKO mice receiving FGF21 or vehicle treatment with saline infusion or Ang II infusion for 28 days. GAPDH was used as a loading control. B) Western blotting showing the expression levels of acetylated-FoxO1, total FoxO1, Catalase, MnSOD and Bim in Ang II treated isolated cardiomyocytes transfected with SIRT1 siRNA or control siRNA followed by treatment with or without FGF21. GAPDH was used as a loading control. C) Quantification of Ac-FoxO1, Catalase, MnSOD and Bim protein levels in different groups of mice ($^{*}P < 0.05$, $^{**}P < 0.01$, N.S., not significant). Data are mean ± SEM for n = 4 mice in each group. D) Quantification of Ac-FoxO1, Catalase, MnSOD and Bim protein levels in different groups of isolated cardiomyocytes ($^{*}P < 0.05$ versus isolated cardiomyocytes transfected with control siRNA, $^{\&}P < 0.05$ versus Ang II treated isolated cardiomyocytes transfected with control siRNA, $^{\#}P < 0.05$ versus Ang II and FGF21 treated isolated cardiomyocytes transfected with control siRNA). E) Immunoprecipitation assays showing the interaction of SIRT1 and FoxO1 in Ang II treated isolated cardiomyocytes transfected with SIRT1 siRNA or control siRNA followed by treatment with or without FGF21.

pathways, including mTOR/p70S6K and eEF2, resulting in reduced protein synthesis, thus alleviating pathological cardiomyocyte growth. AMPK signaling also enhances catabolic pathways, such as glycolysis, to restore the energetic balance required for cell survival [41]. There are several pharmacological agents previously demonstrated to prevent cardiac hypertrophy development, such as AICAR, metformin, and resveratrol, all of which are AMPK activators [24,42,43], as is FGF21. In the present studies, deletion of SIRT1 largely abolished the activation of AMPK by FGF21, at least in part through the regulation of LKB1, suggesting that SIRT1 is a pivotal regulator of FGF21-induced AMPK activation.

In addition to the SIRT1/LKB1/AMPK signaling pathway, other mechanisms may also contribute to FGF21-mediated cardioprotection. For instance, FGF21 also stimulated the expression of catalase and MnSOD, reduced the expression of Bim, and directly lowered oxidative stress and apoptosis in both mouse hearts and cultured cardiomyocytes. As previously reported, SIRT1-mediated deacetylation of FoxO1 directly controls the expression of catalase and MnSOD, whereas hyperacetylated FoxO1 promotes Bim expression and thus apoptosis [25–30]. Our IP assays provide evidence that FGF21 promotes the interaction between SIRT1 and FoxO1, thus altering the transcriptional activity of FoxO1.

Beside the cardioprotective effects of FGF21 on Ang II-induced cardiac hypertrophy and dysfunction, the relationship between FGF21 and hypertension has been clearly identified in previous studies [20,44,45]. One of these researches has also demonstrated that FGF21 could significantly attenuate Ang II-induced hypertension and vascular dysfunction in mice [20]. In our study, recombinant FGF21 helped to lower systolic and diastolic blood pressure in Ang II infusion mouse models. More importantly, we found that FGF21 still had protective effects on the hypertension in SIRT1-iKO mice, and cardiomyocyte-specific SIRT1 knockout did not affect blood pressure both in normal and Ang II infusion conditions. As far as we know, this is the first report to demonstrate cardiomyocyte SIRT1 does not affect the high blood pressure induced by Ang II, especially compared to a previous research which proved that cardiomyocyte mIGF-1/SIRT1 signaling could induce hypertension in mice [46].

Recent studies indicate that FGF21 treatment ameliorates multiple forms of tissue damage, and in different disease models, FGF21 has been shown to alleviate metabolic and cellular insults in diverse tissues [3,5,40,47]. Our results identified the effects of long-term exogenous administration of FGF21 on Ang II-induced cardiac hypertrophy and dysfunction. FGF21 prevented myocardial fibrosis and apoptosis and preserved cardiac function through the regulation of SIRT1 deacetylase activity, and SIRT1 is essential for the protective effects of FGF21 in the heart, but cardiomyocyte SIRT1 does not affect the blood pressure changes altered by Ang II/FGF21 in mice. On the other hand, it is also worth noting that we did not use a large number of animals per group in our research, this does not blunt the statistical significance of differences and reaching conclusions, but might be a limitation of the study. Taken together, these results suggest the possibility that FGF21 act as an effective drug for the treatment of pathological cardiac hypertrophy.

Supplementary data to this article can be found online at https://doi.org/10.1016/j.bbadis.2019.01.019.

## Conflicts of interest

All the authors declare that there are no conflicts of interest in this article.

## Transparency document

The Transparency document associated with this article can be found, in online version.

## Acknowledgements

This work was supported by the National Natural Science Foundation of China (81573069, 81500295, 81570368, 81673077 and 81770498), the Zhejiang Provincial Natural Science Foundation of China (LY13H040010, LY19H040008), the Zhejiang Province Medical and Health Science Program (2018241516, 2019RC054) and Technology Program of Wenzhou (Y20150010).

## References

[1] E. Braunwald, The war against heart failure: the lancet lecture, Lancet 385 (2015) 812–824.
[2] M. Nakamura, J. Sadoshima, Mechanisms of physiological and pathological cardiac hypertrophy, Nat. Rev. Cardiol. 15 (2018) 387–407.
[3] Y. Luo, S. Ye, X. Chen, et al., Rush to the fire: FGF21 extinguishes metabolic stress, metaflammation and tissue damage, Cytokine Growth Factor Rev. 38 (2017) 59–65.
[4] K. Fon Tacer, A.L. Bookout, X. Ding, et al., Research resource: comprehensive expression atlas of the fibroblast growth factor system in adult mouse, Mol. Endocrinol. 24 (2010) 2050–2064.
[5] F.L. Mashili, R.L. Austin, A.S. Deshmukh, et al., Direct effects of FGF21 on glucose uptake in human skeletal muscle: implications for type 2 diabetes and obesity, Diabetes Metab. Res. Rev. 27 (2011) 286–297.
[6] A. Planavila, I. Redondo, E. Hondares, et al., Fibroblast growth factor 21 protects against cardiac hypertrophy in mice, Nat. Commun. 4 (2013) 2019.
[7] H.C. Chang, L. Guarente, SIRT1 and other sirtuins in metabolism, Trends Endocrinol. Metab. 25 (2014) 138–145.
[8] M.D. Chau, J. Gao, Q. Yang, et al., Fibroblast growth factor 21 regulates energy metabolism by activating the AMPK–SIRT1–PGC-1α pathway, Proc. Natl. Acad. Sci. U. S. A. 107 (2010) 12553–12558.
[9] F. Yeung, J.E. Hoberg, C.S. Ramsey, et al., Modulation of NF-kappaB-dependent transcription and cell survival by the SIRT1 deacetylase, EMBO J. 23 (2004) 2369–2380.
[10] E.J. Kim, J.H. Kho, M.R. Kang, et al., Active regulator of SIRT1 cooperates with SIRT1 and facilitates suppression of p53 activity, Mol. Cell 28 (2007) 277–290.
[11] S.A. Khan, A. Sathyanarayan, M.T. Mashek, et al., ATGL-catalyzed lipolysis regulates SIRT1 to control PGC-1α/PPAR-α signaling, Diabetes 64 (2015) 418–426.
[12] F. Lan, J.M. Cacicedo, N. Ruderman, et al., SIRT1 modulation of the acetylation status, cytosolic localization, and activity of LKB1. Possible role in AMP-activated protein kinase activation, J. Biol. Chem. 283 (2008) 27628–27635.
[13] N.R. Sundaresan, V.B. Pillai, M.P. Gupta, Emerging roles of SIRT1 deacetylase in regulating cardiomyocyte survival and hypertrophy, J. Mol. Cell. Cardiol. 51 (2011) 614–618.
[14] M. Vinciguerra, M.P. Santini, C. Martinez, et al., mIGF-1/JNK1/SirT1 signaling confers protection against oxidative stress in the heart, Aging Cell 11 (2012) 139–149.
[15] N.L. Price, A.P. Gomes, A.J. Ling, et al., SIRT1 is required for AMPK activation and the beneficial effects of resveratrol on mitochondrial function, Cell Metab. 15 (2012) 675–690.
[16] Y.J. Hsu, S.C. Hsu, C.P. Hsu, et al., Sirtuin 1 protects the aging heart from contractile dysfunction mediated through the inhibition of endoplasmic reticulum stress-mediated apoptosis in cardiac-specific Sirtuin 1 knockout mouse model, Int. J. Cardiol. 228 (2017) 543–552.
[17] H.L. Cheng, R. Mostoslavsky, S. Saito, et al., Developmental defects and p53 hyperacetylation in Sir2 homolog (SIRT1)-deficient mice, Proc. Natl. Acad. Sci. U. S. A. 100 (2003) 10794–10799.
[18] A.B. Stein, T.A. Jones, T.J. Herron, et al., Loss of H3K4 methylation destabilizes gene expression patterns and physiological functions in adult murine cardiomyocytes, J. Clin. Invest. 121 (2011) 2641–2650.
[19] W. Cong, C. Niu, L. Lv, et al., Metallothionein prevents age-associated cardiomyopathy via inhibiting NF-κB pathway activation and associated nitrative damage to 2-OGD, Antioxid. Redox Signal. 25 (2016) 936–952.
[20] X. Pan, Y. Shao, F. Wu, et al., FGF21 prevents angiotensin II-induced hypertension and vascular dysfunction by activation of ACE2/angiotensin-(1-7) Axis in mice, Cell Metab. 27 (2018) 1323–1337.
[21] M.D. Tallquist, J.D. Molkentin, Redefining the identity of cardiac fibroblasts, Nat. Rev. Cardiol. 14 (2017) 484–491.
[22] L. Zhao, G. Cheng, R. Jin, et al., Deletion of interleukin-6 attenuates pressure overload-induced left ventricular hypertrophy and dysfunction, Circ. Res. 118 (2016) 1918–1929.
[23] Y. Yao, Q. Lu, Z. Hu, et al., A non-canonical pathway regulates ER stress signaling and blocks ER stress-induced apoptosis and heart failure, Nat. Commun. 8 (2017) 133.
[24] R. Gélinas, F. Mailleux, J. Dontaine, et al., AMPK activation counteracts cardiac hypertrophy by reducing O-GlcNAcylation, Nat. Commun. 9 (2018) 374.
[25] M.E. Giannakou, L. Partridge, The interaction between FOXO and SIRT1: tipping the balance towards survival, Trends Cell Biol. 14 (2004) 408–412.
[26] S.A. Reed, P.B. Sandesara, S.M. Senf, et al., Inhibition of FoxO transcriptional activity prevents muscle fiber atrophy during cachexia and induces hypertrophy, FASEB J. 26 (2012) 987–1000.
[27] D.A. Chistiakov, A.N. Orekhov, Y.V. Bobryshev, The impact of FOXO-1 to cardiac pathology in diabetes mellitus and diabetes-related metabolic abnormalities, Int. J.

Cardiol. 245 (2017) 236–244.
[28] S.S. Myatt, J.J. Brosens, E.W. Lam, Sense and sensitivity: FOXO and ROS in cancer development and treatment, Antioxid. Redox Signal. 14 (2011) 675–687.
[29] L. Qiang, A.S. Banks, D. Accili, Uncoupling of acetylation from phosphorylation regulates FoxO1 function independent of its subcellular localization, J. Biol. Chem. 285 (2010) 27396–27401.
[30] D. Shao, P. Zhai, D.P. Del Re, et al., A functional interaction between Hippo-YAP signalling and FoxO1 mediates the oxidative stress response, Nat. Commun. 5 (2014) 3315.
[31] Y. Yang, Y. Zhao, W. Liao, et al., Acetylation of FoxO1 activates Bim expression to induce apoptosis in response to histone deacetylase inhibitor depsipeptide treatment, Neoplasia 11 (2009) 313–324.
[32] V.B. Patel, J.C. Zhong, M.B. Grant, et al., Role of the ACE2/angiotensin 1-7 axis of the renin-angiotensin system in heart failure, Circ. Res. 118 (2016) 1313–1326.
[33] W.C. De Mello, A.H. Danser, Angiotensin II and the heart: on the intracrine renin-angiotensin system, Hypertension 35 (2000) 1183–1188.
[34] J.G. Travers, F.A. Kamal, J. Robbins, et al., Cardiac fibrosis: the fibroblast awakens, Circ. Res. 118 (2016) 1021–1040.
[35] I. Cucoranu, R. Clempus, A. Dikalova, et al., NAD(P)H oxidase 4 mediates transforming growth factor-beta1-induced differentiation of cardiac fibroblasts into myofibroblasts, Circ. Res. 97 (2005) 900–907.
[36] P. Flevaris, S.S. Khan, M. Eren, et al., Plasminogen activator inhibitor type I controls cardiomyocyte transforming growth factor-β and cardiac fibrosis, Circulation 136 (2017) 664–679.
[37] P. Tanajak, S.C. Chattipakorn, N. Chattipakorn, Effects of fibroblast growth factor 21 on the heart, J. Endocrinol. 227 (2015) 13–30.
[38] C.P. Hsu, P. Zhai, T. Yamamoto, et al., Silent information regulator 1 protects the heart from ischemia/reperfusion, Circulation 122 (2010) 2170–2182.
[39] T. Kawashima, Y. Inuzuka, J. Okuda, et al., Constitutive SIRT1 overexpression impairs mitochondria and reduces cardiac function in mice, J. Mol. Cell. Cardiol. 51 (2011) 1026–1036.
[40] Y. Liu, T.T. Wang, R. Zhang, et al., Calorie restriction protects against experimental abdominal aortic aneurysms in mice, J. Exp. Med. 213 (2016) 2473–2488.
[41] J. Heineke, J.D. Molkentin, Regulation of cardiac hypertrophy by intracellular signaling pathways, Nat. Rev. Mol. Cell Biol. 7 (2006) 589–600.
[42] X. Tang, X.F. Chen, N.Y. Wang, et al., SIRT2 acts as a cardioprotective deacetylase in pathological cardiac hypertrophy, Circulation 136 (2017) 2051–2067.
[43] A.Y. Chan, V.W. Dolinsky, C.L. Soltys, et al., Resveratrol inhibits cardiac hypertrophy via AMP-activated protein kinase and Akt, J. Biol. Chem. 283 (2008) 24194–24201.
[44] R.D. Semba, C. Crasto, J. Strait, et al., Elevated serum fibroblast growth factor 21 is associated with hypertension in community-dwelling adults, J. Hum. Hypertens. 27 (2013) 397–399.
[45] C. Zhang, Z. Huang, J. Gu, et al., Fibroblast growth factor 21 protects the heart from apoptosis in a diabetic mouse model via extracellular signal-regulated kinase 1/2-dependent signalling pathway, Diabetologia 58 (2015) 1937–1948.
[46] G. Bolasco, R. Calogero, M. Carrara, et al., Cardioprotective mIGF-1/SIRT1 signaling induces hypertension, leukocytosis and fear response in mice, Aging (Albany NY) 4 (2012) 402–416.
[47] F.M. Fisher, E. Maratos-Flier, Understanding the physiology of FGF21, Annu. Rev. Physiol. 78 (2016) 223–241.